

Enhanced low-energy fluctuations and increasing out-of-plane coherence in vacancy-ordered Na_xCoO_2

P. Lemmens,² V. Gnezdilov,^{1,2} G. J. Shu,³ L. Alff,⁴ C. T. Lin,⁵ B. Keimer,⁵ and F. C. Chou³

¹*Institute for Condensed Matter Physics, TU Braunschweig, D-38106 Braunschweig, Germany*

²*B.I. Verkin Institute for Low Temperature Physics and Engineering, NASU, 61103 Kharkov, Ukraine*

³*Center for Condensed Matter Sciences, National Taiwan University, Taipei 10617, Taiwan*

⁴*Institute of Materials Science, TU Darmstadt, Petersenstrasse 23, D-64287 Darmstadt, Germany*

⁵*Max-Planck-Institute for Solid State Research, Heisenbergstrasse 1, 70569 Stuttgart, Germany*

(Received 28 June 2013; revised manuscript received 23 September 2013; published 27 November 2013)

We report Raman scattering experiments on the strongly correlated electron system Na_xCoO_2 with $x = 0.71$ and ordered Na vacancies. This phase exhibits unusual transport and thermodynamic properties. Furthermore, hydrated samples with the same Co valency are superconducting. Our Raman scattering data reveal pronounced low-energy fluctuations that diverge in intensity at low temperatures. There is a related decrease of the electronic scattering rate Γ from 50 to 3 cm^{-1} . Simultaneous with the evolution of the scattering rate, phonon anomalies point to an increasing out-of-plane coherence of the lattice with decreasing temperature. These observations may indicate the condensation of spin polarons into an unusual, highly dynamic ground state.

DOI: [10.1103/PhysRevB.88.195151](https://doi.org/10.1103/PhysRevB.88.195151)

PACS number(s): 71.30.+h, 71.38.-k, 78.30.-j

I. INTRODUCTION

The layered compound Na_xCoO_2 represents interesting physics due to the interplay of electronic correlations with lattice degrees of freedom.¹ Its electronic phase diagram is exceptionally rich and includes superconductivity, charge as well as magnetic order, and a regime with very large thermopower. One control parameter is given by the Na content x , which changes both the thickness of the CoO_2 layers and the occupation of the Co bands. Going from the extremes of nominal CoO_2 ($x = 0$) to NaCoO_2 ($x = 1$) the Co valence changes formally from Co^{4+} ($3d^5$) with spin $S = 1/2$ to Co^{3+} ($3d^6$) with $S = 0$. With respect to the Co orbitals, this corresponds to t_{2g}^5 and t_{2g}^6 configurations. The e_g orbitals of Co are at higher energies. According to theoretical work,² many of the anomalous properties of Na_xCoO_2 can be understood in a local picture, by considering the effect of hole doping ($x < 1$) on the Co^{4+} site on the lattice symmetry and electronic structure of adjacent Co^{3+} sites. The presence of such a hole shifts the e_g orbitals energetically closer to the t_{2g} states, enhances interatomic hopping, and stabilizes the intermediate-spin ($S = 1$) state on the Co^{3+} ions adjacent to Co^{4+} ions. It has been proposed that these Co^{3+} ions couple antiferromagnetically (AF) in a sea of ferromagnetic (FM) correlations and form spin polarons. Infrared and photoemission spectroscopies provide evidence for a bandwidth renormalization leading to sharp spin polaron bands.² These observations share similarities to effects in three-dimensional (3D) Co-, Mn-, and Ru-based perovskites, two-dimensional (2D) $(\text{La,Sr})_2\text{MnO}_7$, as well as other FM systems in proximity to a metal-insulator transition, e.g. $(\text{Eu,Lu})\text{B}_6$ and EuO .³ We will discuss the implications of the spin-polaron dynamics in Na_xCoO_2 further below and compare it with these systems.

In Na_xCoO_2 , commensurability effects due to Na vacancy ordering exist for $x = 1/3, 1/2, 0.71$, and 0.84 .^{4,5} This is based on the restriction of Na vacancy superlattice formation to di-, tri-, or quadrivacancy ordering perpendicular to the planes. Such ordering minimizes local strain by the Na vacancies.

Therefore, the doping process is not smooth, but evolves with steplike variations.

For $x = 0.71$, the Na vacancy order stabilizes an unusual electronic state that has been termed polaronic or Curie-Weiss metal. Here, the AF ordering observed at higher x (Ref. 6) is suppressed ($T_N \rightarrow 0$) and there is a very large Curie-Weiss contribution to the magnetic susceptibility $\chi(T)$. Transport experiments show a T -linear resistivity $\rho(T)$, a power law in a magnetic field $\rho(H) \sim H^n$ with $1 < n < 1.6$, and a logarithmic divergence of the specific heat at low temperatures. These anomalous properties are attributed to a Fermi surface reconstruction leading to the formation of small pockets for one part of the charge carriers and a localization of the other part of charge carriers in the Na vacancy clusters.⁷ Itinerant and localized electrons thus coexist in a manner resembling some $4f$ and $5f$ electron compounds.⁸ Geometric frustration of localized spin can suppress long-range magnetic order and lead to a spin liquid, as observed, e.g., in Kagome systems. For $\text{Na}_{0.71}\text{CoO}_2$, such a suppression of magnetic ordering is observed,⁹ and the interplay of the localized and itinerant states could realize a novel spin/charge liquid state with unusual criticality for $T \rightarrow 0$ in the sense of a quantum critical point. Unfortunately, to our knowledge, no spectroscopic data of these unusual correlations exists. Also, the regime of fluctuations is limited to the Na vacancy-ordered phase $\text{Na}_{0.71}\text{CoO}_2$. Therefore, its criticality cannot easily be tuned by changing composition. Here, high-pressure experiments could be used. On the other side, the polaronic or Curie-Weiss metal at $x = 0.71$ has the same Co valence as the hydrated composition that shows superconductivity. This is an indirect hint to the unconventional nature of superconductivity in $\text{Na}_{0.35}\text{CoO}_2 \cdot 1.3\text{H}_2\text{O}$.¹⁰

We have performed Raman scattering experiments on phononic and electronic excitations in Na_xCoO_2 to test its critical behavior and the correlation between electronic and lattice degrees of freedom. We focus on two point phases, $x = 0.71$ and 0.84 , that share Na vacancy ordering but differ with respect to the supercell size, charge localization, and

polaron dynamics. From the observation of electronic Raman scattering, a slowing down of the electronic fluctuations and enhanced polarizability with decreasing temperature is deduced. This indicates an unconventional electronic state at low temperatures. Moderate anomalies in frequency and intensity of an out-of-plane phonon point to the importance of out-of-plane coherence for this state.

II. EXPERIMENTAL DETAILS

Raman scattering measurements were performed in quibackscattering geometry using $\lambda = 514.5$ nm Ar⁺ and $\lambda = 532.1$ nm solid state lasers. The laser power of $P < 10$ mW was focused to a $d = 0.1$ -mm-diameter spot on freshly cleaved single-crystal surfaces. Spectra of the scattered radiation were collected via a triple spectrometer (Dilor XY) and recorded by a nitrogen-cooled CCD detector (Horiba Jobin-Yvon, Spectrum One) with a spectral resolution of $\Delta\omega \sim 0.5$ cm⁻¹.

Single crystals and thin films have been prepared by the optical floating-zone growth method under controlled oxygen atmosphere⁴ and by laser ablation, respectively.^{11,12} Using electrochemical techniques as a soft chemical reaction, the Na content of selected single crystals has been tuned to reach equilibrium states at $x = 0.71$ and 0.84 . For extensive experimental characterization, x-Ray diffraction, electrical transport, and superconducting quantum interference device (SQUID) magnetometry has been used.^{4,5} In Raman scattering, the electrochemical equilibration leads to very sharp phonon modes of the respective single crystals. Na vacancy ordering has not been considered in previously published Raman work.^{13,14}

III. RESULTS AND DISCUSSION

The Raman spectrum of Na_xCoO₂ comprises of electronic Raman scattering,¹³ low-frequency sodium as well as higher-frequency oxygen phonon modes.¹⁴⁻¹⁶ In-plane oxygen modes (E_g symmetry, $\omega \sim 450$ cm⁻¹) can be used to probe ordering phenomena in the CoO₂ planes. Co ion charge ordering leads to a multiplication of these modes as observed, e.g. for $x = 0.5$.¹⁶ Out-of-plane oxygen modes (A_{1g} symmetry, $\omega \sim 580$ cm⁻¹) couple strongly to the electronic correlation energy on the Co site.¹⁵ This mode shows a constant frequency for $x < 0.5$ and a linear increase from 570 to 590 cm⁻¹ with $x > 0.5$. In the presently studied Na-vacancy-ordered compositions, we observe two in-plane modes. The frequency of the out-of-plane mode is given by 576.2 and 579.5 cm⁻¹, for $x = 0.71$ and 0.84 , respectively. This is in excellent agreement with earlier studies¹⁴ of the structure property relationship in Na_xCoO₂. Furthermore, we conclude that the Coulomb correlation on Co does not change with vacancy ordering.^{4,5}

In the following, we will focus on electronic Raman scattering, which is observed below the phonon energy. In Fig. 1, Bose-corrected Raman data $\text{Im } \chi(\omega)$ are given. There exists low-energy Raman scattering with an enormous enhancement of intensity toward low temperatures. This effect decisively depends on the type of vacancy ordering, as the sample with $x = 0.84$ has a much smaller related intensity and a less pronounced temperature dependence (inset

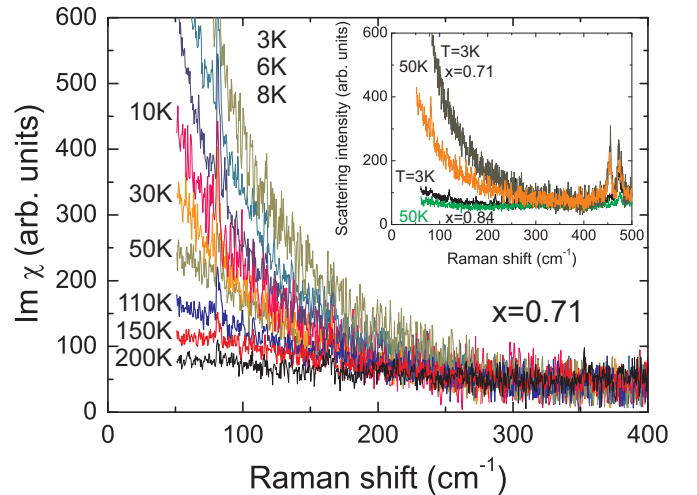


FIG. 1. (Color online) Bose-corrected Raman spectra $\text{Im } \chi(\omega)$ for $x = 0.71$ show a low-energy scattering intensity that diverges in intensity with decreasing temperatures. The inset compares the Raman-scattering intensity at $T = 3$ and 50 K for $x = 0.71$ with $x = 0.84$, respectively. The data evidences a kind of critical behavior at low temperatures for $x = 0.71$.

of Fig. 1). The sample with $x = 0.84$ also shows a much smaller increase of the magnetic susceptibility $\chi(T)$ to low temperatures compared to $x = 0.71$ data.⁵ The inset of Fig. 1 gives the as-measured, non-Bose-corrected data. This proves that the temperature dependence is by no means a consequence of the Bose factor alone. In samples with Na disorder ($x > 0.73$), anomalous low-energy scattering has also been observed. Here, however, a plateau of scattering is observed that extends to higher energies. For $x \leq 1$, even a maximum at $\omega_{\text{max}} = 58$ cm⁻¹ is resolved. This scattering is essentially temperature independent with respect to energy and intensity and has been attributed to collision-dominated, electronic Raman scattering.¹³ The plateau observed in the disordered samples does not appear to be present in vacancy-ordered samples.

In general, low-energy electronic scattering is observed in metals or doped semiconductors only if dominant charge or spin scattering exists. The collision-dominated regime is characterized by a scattering rate Γ that is larger than the product of the Fermi velocity and the scattered momentum $\Gamma > v_F \cdot q$, and the respective scattering intensity is enhanced in proximity to a metal insulator transition.¹⁷ In layered cobaltates, the scattering has been attributed to spin-state polarons or other defect states.¹³ The maximum position of Bose-corrected data is close to the scattering rate of the process $\omega_{\text{max}} \approx \Gamma$. In the parameter range where the Bose factor is not relevant, the line shape of the scattering profile is directly related to Γ . Therefore, Γ can also be determined by a fit to the high-energy shoulder of the data. This is useful if a reduced low-energy resolution or elastic scattering do not allow direct detection of the maximum.

We have performed extensive modeling of our experimental data using Bose-corrected Lorentzian profiles with either $\omega_{\text{max}} = 0$ or $\omega_{\text{max}} \sim \Gamma \neq 0$. An example for the latter fit is shown in Fig. 2 with data at $T = 110$ K. The Bose-corrected Lorentzian with $\omega_{\text{max}} \neq 0$ provides an excellent representation

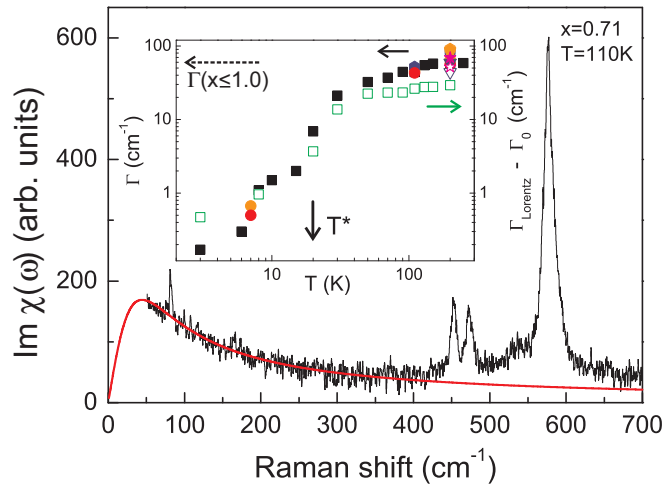


FIG. 2. (Color online) Bose-corrected Raman spectrum for Na vacancy-ordered $x = 0.71$ at $T = 110$ K together with the result of a fit (red line) using a model of collision-dominated scattering. The inset shows the scattering rate Γ as function of temperature on a log-log plot. Data with full symbols correspond to a model of collision-dominated scattering. The dashed arrow gives the temperature-independent Γ of Na disordered samples. Colored symbols show data with higher resolution and a lower-energy onset down to 20 cm^{-1} . Open symbols give the line width $\Gamma_{\text{Lorentz}} - \Gamma_0$ with the offset $\Gamma_0 = 80 \text{ cm}^{-1}$ of a Lorentzian with $\omega_{\text{max}} = 0 \text{ cm}^{-1}$.¹⁸

of the data, although the available frequency window does not allow us to resolve the peak position directly. Here, Γ determined from the high-energy shoulder is strongly temperature dependent. It shows a fast drop and a power law for $T < T^* \sim 20 \text{ K}$, $\Gamma(T) \approx A \cdot T^\alpha$, with $\alpha \sim 2$, see inset of Fig. 2. Such an algebraic dependence implies that the fluctuations are not governed by an energy gap. Otherwise, the temperature dependence would be given by an exponential factor.

The meaning of such fitting could be questioned as Γ turns out to be smaller than the lower-energy cutoff of the Raman data. Therefore, we enhanced the optical resolution of the spectrometer by closing the slit width of the instrument to $\frac{1}{2}$ and $\frac{1}{4}$ of the nominal value ($d = 100 \mu\text{m}$). The low-energy cutoff of the spectrum is now 22 cm^{-1} instead of the previous 50 cm^{-1} . The scattering rates determined from these high-resolution data do not differ by more than 3–7% from those displayed in Fig. 2, depending on temperature. This means that the limited energy resolution has only a small effect on the determination of Γ at low temperatures. For higher temperatures, we observe a saturation of Γ to a value close to the value of Na disordered samples $\Gamma(T > 200 \text{ K}) \approx 60 \text{ cm}^{-1}$. Here, defect-induced electronic scattering dominates. At low temperatures, quasielastic Lorentzians with fixed $\omega_{\text{max}} = 0$ lead to an equally good description of the data. The derived line width Γ_{Lorentz} is shown in the inset of Fig. 2. There is also a strong renormalization observed, albeit somewhat less pronounced than in the alternative analysis scheme presented above. Summarizing our evaluation, the low-energy scattering shows a strong renormalization of the linewidth and therefore of the scattering rate. The temperature-dependent linewidth extracted from the data is only weakly dependent on the model

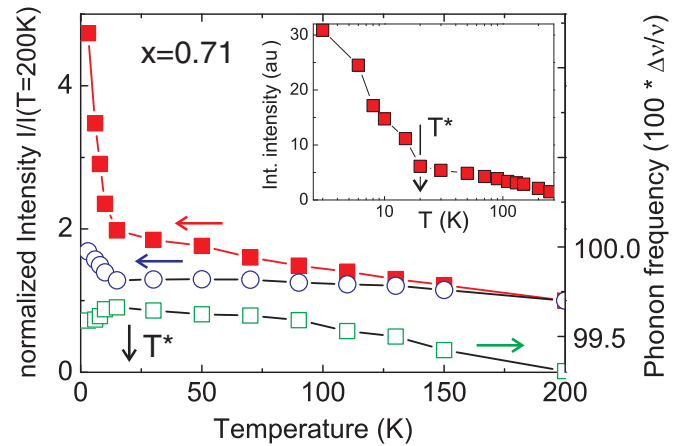


FIG. 3. (Color online) Normalized scattering intensity of the low-energy scattering integrated over the energy window $50\text{--}400 \text{ cm}^{-1}$ (full squares) and the out-of-plane A_{1g} phonon (open circles) scattering together with the A_{1g} phonon frequency shift (open squares, right axis). The inset shows the low-energy scattering intensity data on a logarithmic temperature scale. The latter dependence shows similarities to the specific heat attributed a quantum critical point.⁷

used for analysis and on the restricted frequency window of the experiment.

The intensity of the low-energy scattering exhibits a similarly large variation at low temperatures, see Fig. 3. A change in slope is visible at $T^* = 20 \text{ K}$. The inset of Fig. 3 gives evidence that the low-temperature divergence is close to logarithmic. The intensity is determined from a fit using a Lorentzian and a frequency window from $50\text{--}400 \text{ cm}^{-1}$. This intensity does not depend on the fitting procedure. The observed intensity variation with temperature is also not related to a trivial change of the scattering volume, e.g. via the optical penetration depth or optical constants. This is evident from the invariant intensity of the in-plane phonons that is related to the same geometrical factors, see Fig. 4. We also

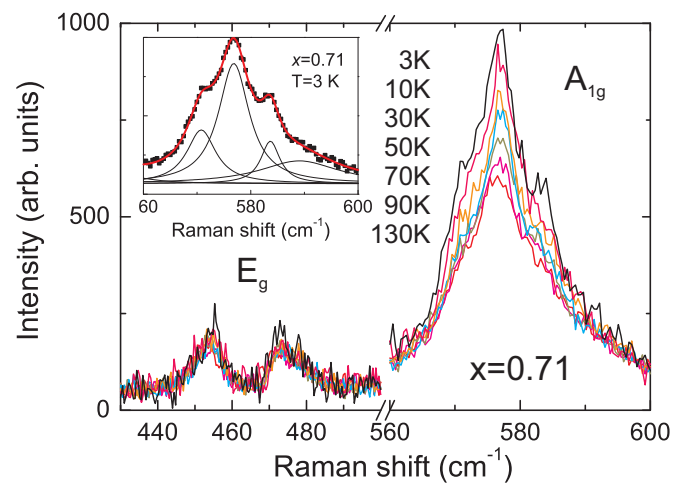


FIG. 4. (Color online) Temperature evolution of the E_g in-plane and A_{1g} out-of-plane modes with a continuous intensity increase of the latter and the development of sidebands. In the inset, the out-of-plane mode is enlarged together with fits to the main and the side bands.

disregard a collective structural change or Co charge ordering in the low-temperature regime as these modes do not change in energy or in number. Therefore, we attribute the intensity gain of the collision-dominated scattering to an enhanced electronic polarizability of the low-temperature state.

The out-of-plane phonon mode shows a gain in intensity and the evolution of two sidebands with decreasing temperature. This effect is smaller than the previously discussed intensity increase of the low-energy electronic scattering. In Fig. 3, the data are compared using open circles with filled squares, respectively. It is interesting to note that neither of these effects saturate at the lowest temperatures. The frequency (open squares) of the out-of-plane phonon mode shows a small softening for $T < T^*$. We attribute the effects of the out-of-plane phonon and side-band evolution to a crossover to a state with higher lattice coherence along the c axis direction. This takes into account that the vacancy ordering in $\text{Na}_{0.71}\text{CoO}_2$ involves staging of defect clusters in this direction.⁵ Comparing the magnitude of the effects, we conclude that structural degrees of freedom are coupled to the low-energy electronic fluctuations but that are not their main driving force. We note that spin polarons discussed in Ref. 2 are indeed expected to couple to the crystal lattice because of the different spatial extent of the Co spin states. Further work is required to assess whether this effect can explain the specific phonon anomalies presented here.

Our Raman-scattering experiments exhibit three major features:

(I) Collision-dominated scattering exists with a scattering rate $\Gamma(T)$ that shows a strong decrease toward low temperatures. The high-temperature limit of $\Gamma(T)$ corresponds to the value of vacancy disordered compounds.

(II) The low-energy scattering intensity $I(T)$ increases strongly with decreasing temperature, without any indication of saturation.

(III) Weaker anomalies are observed in the frequency and intensity of the out-of-plane phonon at T^* .

The crossover temperature T^* with characteristic changes in all data of Fig. 4 coincides with the ordering temperature $T_N = 18\text{--}22$ K of A-type AF order (FM in-plane correlations) observed for disordered samples with $x > 0.75$.⁶ For the vacancy-ordered phase, however, long-range magnetic ordering has been ruled out based on the continuously diverging magnetic susceptibility⁵ and power law in the specific heat.⁷ Nevertheless, samples with larger x and smaller hole content may show an intrinsically inhomogeneous magnetic state with a spin-glass-like freezing of the Co spins at $T_f = 22$ K.¹⁹ Therefore, it seems likely that $T^* = 20$ K for $x = 0.71$ implies a weak change of the spin-spin correlation length. The microscopic origin of this effect remains unclear.

The large reduction of Γ and increase of $I(T)$ appear to be directly related. Indeed, collision-dominated processes with varying peak position and scattering intensity have previously been reported for FM spin-polaron systems, as $\text{Eu}_{1-x}\text{Gd}_x\text{O}$ and $\text{Eu}_{1-x}\text{La}_x\text{B}_6$.¹⁷ Here, maxima exist with scattering rates varying in the range of $\Gamma = 20\text{--}45$ cm^{-1} and $5\text{--}8.5$ cm^{-1} , respectively, and are attributed to a metal-insulator transition with enhanced spin-polaron dynamics.¹⁷ In these systems, a scaling of $\Gamma(T) \sim \chi \cdot T$ has been observed. This is due to the dominance of spin fluctuations in the scattering processes that

leads to a mean free path $l = \chi \cdot T$. In the regime of increasing scattering rates also, the scattering intensities show a moderate gain.

These cases show some similarities with $\text{Na}_{0.71}\text{CoO}_2$, i.e. in-plane correlations are FM and spin-orbital polarons have been discussed. However, from $\chi(T) \approx C/T$ in the Curie-Weiss metal $\text{Na}_{0.71}\text{CoO}_2$, a constant, temperature-independent scattering rate Γ would be expected. Also, the temperature variations are opposite: In $\text{Na}_{0.71}\text{CoO}_2$, the decreasing $\Gamma(T)$ is accompanied by an increasing $I(T)$. The decreasing $\Gamma(T)$, on the other side, is consistent with the relatively smaller and T -linear resistivity that marks anomalous electronic correlations.^{5,7} These observations could point back to the origin of the local moments, a localization of charge carriers to $S = 1/2$ magnetic moments within vacancy clusters, and a concomitant restructuring of the Fermi surface to small pockets. The decreasing scattering rate would then be related to a decreasing density of spin-polaron states and the increasing electronic scattering intensity to a rather dynamic and highly polarizable low energy state. The major difference between $\text{Na}_{0.71}\text{CoO}_2$ on the one hand and materials such as $\text{Eu}_{1-x}\text{Gd}_x\text{O}$ on the other hand is that the latter show FM order while the former does not exhibit long-range order, probably as a consequence of frustrated interactions. The suppression of long-range order together with enhanced fluctuations for $T \rightarrow 0$ are hints to the existence of a quantum critical point.⁹

Usually electron-phonon coupling leads to instabilities that suppress fluctuations, by opening an excitation gap. For the $x = 0.71$ phase, this is not the case. Reasons for the ineffectiveness of electron-phonon coupling are probably related to the complex vacancy cluster ordering that may lead to frustrated magnetostructural interactions. Furthermore, the out-of-plane phonon couples mainly to momenta at the center of the Brillouin zone.¹⁵ It is thereby ineffective to trigger a collective lattice instability that would alter the electronic fluctuations.

Finally, we briefly mention a possible relevance of the dynamic low-temperature state of $\text{Na}_{0.71}\text{CoO}_2$ for the superconducting, hydrated compositions. Hydration of $\text{Na}_{0.3}\text{CoO}_2 \cdot 1.4 \text{H}_2\text{O}$ leads to the intercalation of additional layers separating and decoupling the CoO_2 planes. This composition has a Co valence that is very close to the present one in $\text{Na}_{0.71}\text{CoO}_2$, which implies that the enhanced fluctuations are of relevance for superconductivity.¹⁰ For this composition, anomalous electronic scattering processes have also been inferred from transport experiments.²⁰ On the other side, electronic Raman scattering for this composition shows a smaller intensity at low temperatures and a gap formation. This gives evidence that Raman scattering in this case is dominated by a different scattering mechanism and is not dominated by a collision-dominated response.

Summarizing, using Raman scattering, we give evidence for a regime of pronounced fluctuations for temperatures below $T^* = 20$ K in the Na vacancy-ordered cobaltate $\text{Na}_{0.71}\text{CoO}_2$. Experimentally, this is based on the observation of a strongly reduced electronic scattering rate and a diverging scattering intensity. The latter corresponds to an enlarged electronic polarizability. $\text{Na}_{0.71}\text{CoO}_2$ differs from other compositions by a suppressed long-range magnetic order, anomalous transport and thermodynamic properties, and a restructured Fermi

surface with a partial localization of charge carriers at vacancy clusters. The observed electronic Raman scattering is interpreted as collision-dominated scattering due to spin polarons. Spin polarons could play some role for the proposed quantum critical point. Finally, we point out that the existence range of this phase with anomalous fluctuations can be shifted to a different Na composition ($x = 2/3$) inducing oxygen defects while keeping the Co valence constant.²¹ This is consistent with the dominance of electronic correlations over structural effects related to the Na vacancy ordering. Theoretical studies

of the stability of Na vacancy-ordered phases²² as well as on the combination of disorder and correlations on the thermopower²³ have come to similar conclusions.

ACKNOWLEDGMENTS

We acknowledge important discussion with P. A. Lee, S. L. Cooper, and D. Wulferding. This work was supported by Deutsche Forschungsgemeinschaft (DFG AL560/6, KE923/2, LE967/4).

-
- ¹D. J. Singh, *Phys. Rev. B* **61**, 13397 (2000); M. Roger, D. J. P. Morris, D. A. Tennant, M. J. Gutmann, J. P. Goff, J.-U. Hoffmann, R. Feyerherm, E. Dudzik, D. Prabhakaran, A. T. Boothroyd, N. Shannon, B. Lake, and P. P. Deen, *Nature* **445**, 631 (2007); H. Li, R. T. Clay, and S. Mazumdar, *Phys. Rev. Lett.* **106**, 216401 (2011); N. B. Ivanova, S. G. Ovchinnikov, M. M. Korshunov, I. M. Eremin, and N. V. Kazak, *Phys.-Usp.* **52**, 789 (2009).
- ²J. Chaloupka and G. Khaliullin, *Prog. Theor. Phys. Suppl.* **176**, 50 (2008); M. Daghofer, P. Horsch, and G. Khaliullin, *Phys. Rev. Lett.* **96**, 216404 (2006); J. Chaloupka and G. Khaliullin, *ibid.* **99**, 256406 (2007); G. Khaliullin and J. Chaloupka, *Phys. Rev. B* **77**, 104532 (2008); C. Bernhard, A. V. Boris, N. N. Kovaleva, G. Khaliullin, A. V. Pimenov, Li Yu, D. P. Chen, C. T. Lin, and B. Keimer, *Phys. Rev. Lett.* **93**, 167003 (2004).
- ³S. L. Cooper, in *Structure and Bonding*, edited by J. B. Goodenough (Springer-Verlag, Berlin, Heidelberg, 2001), Vol. 98, p. 163.
- ⁴G. J. Shu, A. Prodi, S. Y. Chu, Y. S. Lee, H. S. Sheu, and F. C. Chou, *Phys. Rev. B* **76**, 184115 (2007); G. J. Shu and F. C. Chou, *ibid.* **78**, 052101 (2008).
- ⁵F. C. Chou, M.-W. Chu, G. J. Shu, F.-T. Huang, W. Wu Pai, H. S. Sheu, and P. A. Lee, *Phys. Rev. Lett.* **101**, 127404 (2008).
- ⁶S. P. Bayrakci, I. Mirebeau, P. Bourges, Y. Sidis, M. Enderle, J. Mesot, D. P. Chen, C. T. Lin, and B. Keimer, *Phys. Rev. Lett.* **94**, 157205 (2005).
- ⁷L. Balicas, Y. J. Jo, G. J. Shu, F. C. Chou, and P. A. Lee, *Phys. Rev. Lett.* **100**, 126405 (2008); A. Zorkovská, A. Baran, M. Kajňáková, A. Feher, J. Šebek, E. Šantavá, C. T. Lin, and J. B. Peng, *Phys. Status Solidi B* **247**, 665 (2010).
- ⁸G. Zwirgagl and P. Fulde, *J. Phys.: Condens. Matter* **15**, S1911 (2003); D. V. Efremov, N. Hasselmann, E. Runge, P. Fulde, and G. Zwirgagl, *Phys. Rev. B* **69**, 115114 (2004).
- ⁹H. Alloul, I. R. Mukhamedshin, T. A. Platova, and A. V. Dooglav, *Europhys. Lett.* **85**, 47006 (2009).
- ¹⁰H. Ohta, K. Yoshimura, Z. Hu, Y. Y. Chin, H.-J. Lin, H. H. Hsieh, C. T. Chen, and L. H. Tjeng, *Phys. Rev. Lett.* **107**, 066404 (2011).
- ¹¹Y. Krockenberger, I. Fritsch, G. Cristiani, H.-U. Habermeier, Li Yu, C. Bernhard, B. Keimer, and L. Alff, *Appl. Phys. Lett.* **88**, 162501 (2006); L. Yu, L. Gu, Y. Wang, P. X. Zhang, and H.-U. Habermeier, *J. Cryst. Growth* **328**, 34 (2011).
- ¹²L. Alff, A. Klein, Ph. Komissinskiy, and J. Kurian, in *Ceramics Science and Technology, Volume 3: Synthesis and Processing*, edited by I.-W. Chen and R. Riedel (Wiley-VCH Verlag GmbH, Weinheim, Germany, 2011), pp. 269–290.
- ¹³P. Lemmens, K.-Y. Choi, V. Gnezdilov, E. Ya. Sherman, D. P. Chen, C. T. Lin, F. C. Chou, and B. Keimer, *Phys. Rev. Lett.* **96**, 167204 (2006).
- ¹⁴T. Wu, K. Liu, H. Chen, G. Wu, Q. L. Luo, J. J. Ying, and X. H. Chen, *Phys. Rev. B* **78**, 115122 (2008); H. X. Yang, Y. Xia, Y. G. Shi, H. F. Tian, R. J. Xiao, X. Liu, Y. L. Liu, and J. Q. Li, *ibid.* **74**, 094301 (2006); J. F. Qu, W. Wang, Y. Chen, G. Li, and X. G. Li, *ibid.* **73**, 092518 (2006); P. Lemmens, P. Scheib, Y. Krockenberger, L. Alff, F. C. Chou, C. T. Lin, H.-U. Habermeier, and B. Keimer, *ibid.* **75**, 106501 (2007); M. N. Iliev, A. P. Litvinchuk, R. L. Meng, Y. Y. Sun, J. Cmaidalka, and C. W. Chu, *Physica C* **402**, 239 (2004); A. Semenova, D. Kellermana, I. Baklanovaa, L. Perelyaevaa, and E. Vovkotrub, *Chem. Phys. Lett.* **491**, 169 (2010), and references therein.
- ¹⁵A. Donkov, M. M. Korshunov, I. Eremin, P. Lemmens, V. Gnezdilov, F. C. Chou, and C. T. Lin, *Phys. Rev. B* **77**, 100504(R) (2008).
- ¹⁶X. N. Zhang, P. Lemmens, B. Keimer, D. P. Chen, C. T. Lin, K. Y. Choi, V. Gnezdilov, and F. C. Chou, *Physica B* **359–361**, 424 (2005); Q. Zhang, M. An, Sh. Yuan, Y. Wu, D. Wu, J. Luo, N. Wang, W. Bao, and Y. Wang, *Phys. Rev. B* **77**, 045110 (2008).
- ¹⁷H. Rho, C. S. Snow, S. L. Cooper, Z. Fisk, A. Comment, and J. Ph. Ansermet, *Phys. Rev. Lett.* **88**, 127401 (2002); C. S. Snow, S. L. Cooper, D. P. Young, Z. Fisk, A. Comment, and J. Ph. Ansermet, *Phys. Rev. B* **64**, 174412 (2001).
- ¹⁸The offset Γ_0 is chosen to give an overlap of the scattering rates at low temperatures, as shown in Fig. 2.
- ¹⁹C. Bernhard, Ch. Niedermayer, A. Drew, G. Khaliullin, S. Bayrakci, J. Stremper, R. K. Kremer, D. P. Chen, C. T. Lin, and B. Keimer, *Europhys. Lett.* **80**, 27005 (2007).
- ²⁰G. Cao, M. M. Korshunov, Y. Gao, M. Le Tacon, D. J. Singh, and C.-T. Lin, *Phys. Rev. Lett.* **108**, 236401 (2012).
- ²¹G. J. Shu, W. L. Lee, F.-T. Huang, M.-W. Chu, Patrick A. Lee, and F. C. Chou, *Phys. Rev. B* **82**, 054106 (2010).
- ²²Y. Wang, Y. Ding, and J. Ni, *J. Phys.: Condens. Matter* **21**, 035401 (2009).
- ²³P. Wissgott, A. Toschi, G. Sangiovanni, and K. Held, *Phys. Rev. B* **84**, 085129 (2011).